REPORT DOCUMENTATION PAGE

Form Approved OMB NO. 0704-0188

1. REPORT DATE (DD-MM-YYYY)	2. REPORT TYPE	3. DATES COVERED (From - To)
01-11-2010	Final Report	25-Aug-2006 - 24-Aug-2010

4. TITLE AND SUBTITLE

Electrically tunable mid-infrared single-mode high-speed semiconductor laser

5a. CONTRACT NUMBER
W911NF-06-1-0399

5b. GRANT NUMBER

5c. PROGRAM ELEMENT NUMBER
611102

6. AUTHORS

Gregory Belenky, Sergey Suchalkin

5d. PROJECT NUMBER

5e. TASK NUMBER

5f. WORK UNIT NUMBER

7. PERFORMING ORGANIZATION NAMES AND ADDRESSES

Research Foundation of State University of New
Office of Sponsored Programs
Research Foundation Of SUNY
Stony Brook, NY 11794 -3362

8. PERFORMING ORGANIZATION REPORT NUMBER

9. SPONSORING/MONITORING AGENCY NAME(S) AND ADDRESS(ES)

U.S. Army Research Office
P.O. Box 12211
Research Triangle Park, NC 27709-2211

10. SPONSOR/MONITOR'S ACRONYM(S)
ARO

11. SPONSOR/MONITOR'S REPORT NUMBER(S)
49627-EL.3

12. DISTRIBUTION AVAILIBILITY STATEMENT

Approved for Public Release; Distribution Unlimited

13. SUPPLEMENTARY NOTES

The views, opinions and/or findings contained in this report are those of the author(s) and should not contrued as an official Department of the Army position, policy or decision, unless so designated by other documentation.

14. ABSTRACT

Single mode tunable mid-IR semiconductor lasers are in high demand in chemical sensing, pollution monitoring, industrial process control and optical communications. Working on the project we proposed and proved theoretically the way of rapid electrical tuning of mid-IR semiconductor lasers. We also developed the mid-IR laser design and pushed the long wavelength limit of CW room temperature operation to 3.4nm for type I GaSb based quantum well lasers. A single lateral mode laser emitting CW at 3.15um at room temperature was demonstrated.

15. SUBJECT TERMS

tunable laser, cascade laser, mid-IR laser

16. SECURITY CLASSIFICATION OF:			17. LIMITATION OF ABSTRACT	15. NUMBER OF PAGES	19a. NAME OF RESPONSIBLE PERSON
a. REPORT	b. ABSTRACT	c. THIS PAGE			Gregory Belenky
UU	UU	UU	UU		19b. TELEPHONE NUMBER: 631-632-8397

Report Title

Electrically tunable mid-infrared single-mode high-speed semiconductor laser

ABSTRACT

Single mode tunable mid-IR semiconductor lasers are in high demand in chemical sensing, pollution monitoring, industrial process control and optical communications. Working on the project we proposed and proved theoretically the way of rapid electrical tuning of mid-IR semiconductor lasers. We also developed the mid-IR laser design and pushed the long wavelength limit of CW room temperature operation to 3.4nm for type I GaSb based quantum well lasers. A single lateral mode laser emitting CW at 3.15um at room temperature was demonstrated. This device is an important step towards development of a continuously tunable single mode mid-IR laser operating above 3um at room temperature.

List of papers submitted or published that acknowledge ARO support during this reporting period. List the papers, including journal references, in the following categories:

(a) Papers published in peer-reviewed journals (N/A for none)

1. M. V. Kisin, M. Dutta, and M. A. Stroscio, "Eectron-phonon interactions in intersubband laser heterostructures," in Advanced Semiconductor Heterostructures: Novel Devices, Potential Device Applications and Basic Properties. vol. 28 Singapore: World Scientific, 2003, pp. 1-30.
2. M. V. Kisin, B. L. Gelmont, and S. Luryi, "Boundary-condition problem in the Kane model," Physical Review B, vol. 58, pp. 4605-4616, Aug 15 1998.
3. D.Westerfeld, S.Suchalkin, M.Kisin, G.Belenky, J.Bruno, R.Tober, “Experimental study of optical gain and loss in 3.4-3.6 mu m interband cascade lasers”, IEE Proc.-Optoelectron., 150, 293 (2003).
4. M. V. Kisin, S. D. Suchalkin, and G. Belenky, "Stark effect tunable QCL," in International Conference on Intersubband Transitions in Quantum Wells ITQW’2005, North Falmouth, MA, USA, 2005.
5. S. Suchalkin, M. V. Kisin, S. Luryi, G. Belenky, F. J. Towner, J. D. Bruno, C. Monroy, and R. L. Tober, "Widely tunable type-II interband cascade laser," Applied Physics Letters, vol. 88, pp. 031103-3 (2006).
6. S.Suchalkin, M.V.Kisin, S.Luryi, G.Belenky, J.Bruno, F.J.Towner, R.Tober, "High-speed Stark wavelength tuning of mid-IR interband cascade lasers", IEEE Photonic Technol. Lett., v.19, No5-8, 360 (2007)
7. L.Shterengas, G.Belenky, G.Kipshidze, and T.Hosoda, "Room temperature operated 3.1mm type I GaSb-based diode lasers with 80mW continuous-wave output power," Appl. Phys. Lett., 92, 171111 (2008).
8. L.Shterengas, G.Belenky, T.Hosoda, G.Kipshidze, and, S.Suchalkin "Continuous wave operation of diode lasers at 3.36?m at 12oC," Appl. Phys. Lett., 93, 011103(2008).
9. J.Chen, D.Donetsky, L.Shterengas, M.Kisin, G.Kipshidze, and G.Belenky, "Effect of quantum well compressive strain above 1% on differential gain and threshold current density in type-I GaSb-based diode lasers," IEEE Journ. of Quant. Electron., 44, pp.1204-1210(2008).

Number of Papers published in peer-reviewed journals: 9.00

(b) Papers published in non-peer-reviewed journals or in conference proceedings (N/A for none)

Number of Papers published in non peer-reviewed journals: 0.00

(c) Presentations

1. G.Belenky, L.Shterengas, G.Kipshidze, T.Hosoda, and S. Suchalkin (invited) “CW operated type I GaSb-based diode lasers with wavelength above 3 ?m” MIOMD-IX, St.Petersburg, Russia, 2008.
2. S.Suchalkin, D.Westrefeld, G.Kipshidze, Seungyong Jung, L.Shterengas, T.Hosoda, and G.Belenky, “CW operated type I GaSb-based diode lasers with wavelength above 3 ?m” SPIE Defence and Security, Orlando, FL, 2008.
3. G.Belenky, L.Shterengas, G.Kipshidze, T.Hosoda, S. Suchalkin, “Advances in the development of the GaSb-based laser diodes operating within spectral range of 2 – 3.5 ?m”, 21st Annual Meeting of the IEEE Lasers and Electro-Optics Society, LEOS, 2008.
4. L.Shterengas; G. Kipshidze, T. Hosoda, D. Donetsky, G.Belenky, “Room temperature operated 3.1-?m type-I GaSb-based diode lasers with 80mW continuous wave output power”, Conference on Lasers and Electro-Optics, 2008 and 2008 Conference on Quantum Electronics and Laser Science. CLEO/QELS 2008.
5. G.Belenky, L.Shterengas, G.Kipshidze, T.Hosoda, J. Chen, S. Suchalkin, “GaSb-based laser diodes operating within spectral range of 2 – 3.5 μm”, Lasers and Electro-Optics, 2009 and 2009 Conference on Quantum electronics and Laser Science Conference. CLEO/QELS 2009
6. L.Shterengas, D. Donetsky, M. Kisin, G.Belenky “Carrier capture and recombination in 2.4?m GaSb-based type-I quantum well high power diode lasers”, Quantum Electronics and Laser Science Conference, QELS, 2007.
7. L.Shterengas, D. Donetsky, M. Kisin, G.Belenky “Carrier capture and recombination in 2.4?m GaSb-based type-I quantum well high power diode lasers”, Conference on Lasers and Electrooptics, 2007
8. S.Suchalkin, M.V.Kisin, S.Luryi, G.Belenky, J.Bruno, F.J.Towner, R.Tober, (invited) "Electrically tunable cascade laser" Optics East, Boston, 2006.
9. M.V. Kisin, S. Suchalkin, G. Belenky, "Stark effect tunable QCL", 8th International Conference on Intersubband Transitions in Quantum Wells ITQW’2005, North Falmouth, MA, 2005.

Number of Presentations: 9.00

Non Peer-Reviewed Conference Proceeding publications (other than abstracts):

Number of Non Peer-Reviewed Conference Proceeding publications (other than abstracts): 0

Peer-Reviewed Conference Proceeding publications (other than abstracts):

Number of Peer-Reviewed Conference Proceeding publications (other than abstracts): 0

(d) Manuscripts

Number of Manuscripts: 0.00

Patents Submitted

1.Semiconductor light source with electrically tunable emission wavelength, Belenky, Gregory ; Bruno, John D; Kisin, Mikhail V; Luryi, Serge ; Shterengas, Leon ; Suchalkin, Sergey ; Tober, Richard L
20060056466

Patents Awarded

1.Semiconductor light source with electrically tunable emission wavelength, Belenky, Gregory ; Bruno, John D; Kisin, Mikhail V; Luryi, Serge ; Shterengas, Leon ; Suchalkin, Sergey ; Tober, Richard L
20060056466

Graduate Students

NAME	PERCENT SUPPORTED
Takashi Hosoda	0.50
Ding Wang	0.50
FTE Equivalent:	**1.00**
Total Number:	**2**

Names of Post Doctorates

NAME	PERCENT_SUPPORTED
Gene Tsvid	0.50
FTE Equivalent:	**0.50**
Total Number:	**1**

Names of Faculty Supported

NAME	PERCENT_SUPPORTED	National Academy Member
Gregory Belenky	0.20	No
Leon Shterengas	0.20	No
Sergey Suchalkin	0.40	No
FTE Equivalent:	**0.80**	
Total Number:	**3**	

Names of Under Graduate students supported

NAME	PERCENT_SUPPORTED
FTE Equivalent:	
Total Number:	

Student Metrics

This section only applies to graduating undergraduates supported by this agreement in this reporting period

The number of undergraduates funded by this agreement who graduated during this period:	0.00
The number of undergraduates funded by this agreement who graduated during this period with a degree in science, mathematics, engineering, or technology fields:	0.00
The number of undergraduates funded by your agreement who graduated during this period and will continue to pursue a graduate or Ph.D. degree in science, mathematics, engineering, or technology fields:	0.00
Number of graduating undergraduates who achieved a 3.5 GPA to 4.0 (4.0 max scale):	0.00
Number of graduating undergraduates funded by a DoD funded Center of Excellence grant for Education, Research and Engineering:	0.00
The number of undergraduates funded by your agreement who graduated during this period and intend to work for the Department of Defense	0.00
The number of undergraduates funded by your agreement who graduated during this period and will receive scholarships or fellowships for further studies in science, mathematics, engineering or technology fields:	0.00

Names of Personnel receiving masters degrees

NAME
Total Number:

Names of personnel receiving PHDs

NAME
Total Number:

Names of other research staff

NAME	PERCENT_SUPPORTED
FTE Equivalent:	
Total Number:	

Sub Contractors (DD882)

Inventions (DD882)

Table of Contents

Statement of the Problem Studied and Description of the Results

Single mode tunable mid-IR semiconductor lasers are in high demand in chemical sensing, pollution monitoring, industrial process control and optical communications. The proposed new concept of tunable single-mode cascade laser for mid-infrared applications was realized on the Interband Cascade Laser platform. The key idea is to incorporate in each stage of a quantum cascade laser a charge accumulation region located outside of the optically active quantum wells. The accumulation region should include a QW structure with specially designed intersubband polarization transition which allows electrical control over the modal refractive index and provides a mechanism for fast single-mode laser wavelength tunability. Currently, the most promising optical source in the mid-infrared range is the quantum-cascade laser (QCL). The emission wavelength of a QCL can be tuned to some extent by electrical heating in the laser active region [1]. Direct electrical tuning of the optical transition by the Stark effect remains an unsolved problem in QCL because, after the laser threshold is reached, the carrier concentration in the optically active quantum wells (QWs) becomes clamped according to the threshold condition (gain equals loss) and, therefore, is not changed as the bias current increases. The concentration clamping pins the electric field in the active region to its threshold value thus preventing Stark tuning of the lasing transition. Concentration clamping in the active region can be circumvented by using a multi-sectioned laser design with separate electrical control over the optical gain in each section [2]. In this approach, the optical gain from the additional section modifies the threshold condition in the main lasing section, so that the threshold concentration in the active QWs can be altered. The unclamped concentration of carriers in the active QWs, however, still does not provide direct electrical control over the QCL modal refractive index and, hence, does not ensure single-mode tunable operation. Indeed, the highly symmetrical shape of the intersubband gain/absorption spectrum implies zero index change at the spectrum peak (*i.e.* negligible QCL alpha-factor) which prevents controlling the refractive index by changing the electron concentration in the active QWs.

In order to achieve an electrical control over the modal refractive index, we propose incorporating in each QCL cascade a double-quantum-well (DQW) accumulation region located outside the optically active QWs of the laser. The outside accumulation of electric charge is not clamped by the threshold condition and can be altered by the bias injection current [3]. The DQW structure in the accumulation region is specially designed to provide an intersubband polarization transition shifted in frequency from the main lasing mode of the QCL. The overall gain spectrum thus becomes asymmetrical and allows for non-zero alpha factor at lasing wavelength. In our tuning scheme, the refractive index change of the TM-polarized QCL optical mode at the lasing frequency due to intersubband carrier polarization in the accumulation region is directly related to the accumulated carrier concentration and, therefore, can be controlled by the injection current.

To quantify the main physical processes employed in our tuning scheme we consider a QCL heterostructure with a spatially vertical (intra-well) lasing transition **2-1** in the optically active QW; see Figure 1. Outside carrier accumulation in such a structure will not provoke a strong first-order Stark shift of the whole optical gain spectrum, which would lead to

discontinuous tuning and longitudinal mode hopping in lasers with spatially indirect lasing transition [3, 4]. The DQW accumulation region is separated from the stage's first optically active QW by a special accumulation barrier; see Figure 1. At low bias, this barrier should allow enough injection to reach the laser threshold. After the threshold has been reached, it should provide for efficient carrier accumulation in the accumulation DQW by satisfying the accumulation condition $\tau_{32} > \tau_{21}$. Both requirements can be met by employing LO-phonon assisted carrier transport from the accumulation region to the upper lasing states in the active QWs (injection transition **3-2)**. The characteristic time τ_{32} for this transition is determined by the LO-phonon emission rate [5]:

$$\tau_{32}^{-1} \approx \pi\omega_{LO} \frac{I(q)}{qa_B}; \qquad a_B = \frac{4\pi\varepsilon_0\varepsilon\hbar^2}{m^* e^2}. \tag{1}$$

In our example calculations we consider a low-temperature operation regime with only spontaneous phonon emission in all phonon-assisted transitions; a_B is the effective Bohr radius, and *I(q)* is the electron-phonon overlap integral which, as calculation shows, is not much affected by the injection current below threshold. On the other hand, the momentum $q = \sqrt{2m^*\Delta}/\hbar$ transferred in this transition by the emitted optical phonon noticeably depends on the excess energy $\Delta = E_{32} - \hbar\omega_{LO}$, which increases with injection current due to the increment of the Stark field in the accumulation barrier region, $\Delta F_{32} = eN_3/\varepsilon_0\varepsilon$. This additional electric field is induced by the electron concentration N_3 accumulated in level **3** of the accumulation DQW. The resulting increase in the transition time τ_{32} boosts the process of outside charge accumulation in level **3** which, in turn, further increases the excess energy Δ of the injection transition **3-2**.

The process of outside carrier accumulation described above allows efficient control over the modal refractive index and, therefore, over the position of the optical waveguide comb modes. In interband (type-II) cascade lasers (ICL), characterized by the prevailing TE-polarization of the main optical mode, the 2D free-carrier plasma effect associated with controlled carrier accumulation in the accumulation region is the most straightforward mechanism for modal refractive index control. The real part of the refractive index change incurred by the in-plane *intrasubband* carrier polarization in the accumulation region of an ICL is negative and causes a laser comb-mode shift in the same direction as the Stark shift of the cavity gain spectra observed in ICLs [3]. In QCLs, where the optical mode is TM-polarized with the electric field transverse to the QCL layers, the *intersubband* polarization of the quantum confined carriers in the accumulation DQW should be considered for this purpose instead. Care should be taken to ensure that the intersubband polarization transition is properly detuned from the main optical transition, firstly, to obtain a non-zero alpha-factor at lasing wavelength and, hence, to achieve modal refractive index control, and, secondly, to avoid excessive optical absorption at this wavelength. In our example, we design the accumulation region as a double-QW (DQW) heterostructure with two energy levels **3** and **4**; see Figure 1. The lower level **3** participates in carrier accumulation and subsequent phonon-assisted carrier injection into the active QWs. This level is adjusted by the widths of the DQW and accumulation barrier layers to satisfy the LO-phonon assisted injection condition $E_3 - E_2 \geq \hbar\omega_{LO}$. The position of energy level **4** is adjusted by the intermediate DQW barrier

width d_{34} to provide proper shift of the **3-4** transition energy E_{43} from the energy of lasing transition E_{21}. Assuming a Lorentzian line-shape with broadening parameter γ, the modal index change and additional optical loss induced by the **3-4** polarization transition at the frequency of the lasing transition E_{21} are

$$\Delta n_m = \frac{1}{2} n_m \Gamma N_3 \frac{e^2 z_{34}^2}{\varepsilon_0 \varepsilon} \frac{E_{43} - E_{21}}{(E_{43} - E_{21})^2 + \gamma^2}; \quad (2)$$

$$\alpha = \frac{n_m \omega}{c_0} \Gamma N_3 \frac{e^2 z_{34}^2}{\varepsilon_0 \varepsilon} \frac{\gamma}{(E_{43} - E_{21})^2 + \gamma^2}. \quad (3)$$

Here, Γ is the confinement factor for the accumulation region, and ez_{34} is the dipole matrix element for the polarization transition.

Figure 2 shows the calculated change in the modal refractive index for our structure. The wave functions presented in Figure 1, the overlap integrals, and dipole matrix elements ez_{32} and ez_{21} for the corresponding transitions were obtained by solving the 8-band Schrödinger equation fully accounting for nonparabolicity and band mixing effects in the QWs [5, 6]. Material parameters of $Ga_{0.47}In_{0.53}As/Al_{0.48}In_{0.52}As$ were used for this calculation [7]. Bias current was assumed to be dominated by phonon-assisted non-radiative transitions (1). For clarity of presentation, the injection current in Figure 2 was normalized to the threshold value calculated for a total optical loss of $\alpha = 40$ cm^{-1}. The standard expression for QCL optical gain analogous to Eq. (3) was used to estimate the threshold. For a 30-cascade structure the threshold current was in the range of 1.2-1.5 kA/cm^{-2}. Electron accumulation in level **3** critically depends on the accumulation barrier width d_{32}. Structure 1 with a narrow accumulation barrier maintains the **3-2** anticrossing gap E_{32} to be in resonance with the LO phonon energy $\hbar\omega_{LO}$ with detuning Δ less than the phonon energy over the full range of injection currents. The **3-2** transition rate, therefore, is high enough and charge accumulation in the accumulation region is low (curve 1). For structures with wider accumulation barriers, due to the wider spatial separation of the initial and final states in the phonon-assisted injection transition **3-2**, the transition is more susceptible to the Stark shift and the energy separation E_{32} goes off the LO-phonon resonance with increasing current. In these structures, the outside carrier accumulation drastically increases with current (curves 2-4, inset) as does the index change. This process is self-sustained and, in contrast to the resonant tunneling process, stable [2]. It terminates when higher states in the active QWs become available for electron tunneling escape from the accumulation region.

Figure 2 shows that the intersubband polarization transition embedded in the accumulation region provides efficient control over the refractive index of the TM lasing mode. For an index change of about $\Delta n = 4\times10^{-3}$ corresponding to an injection current increase about $0.1J_{th}$ (line 4 in Figure 2) and for modal index $n = 3.2$ the resulting tuning range is about $\Delta\lambda = \lambda\Delta n / n = 10$ nm. It is interesting that the additional optical loss (3), associated with the polarization transition **3-4**, requires additional injection which, in turn, participates in laser tuning. This mechanism is similar to that discussed in Ref. [2], though in our case the laser design benefits from the fact that regions with controlled losses are embedded in active cascades and, therefore, do not require additional longitudinal integration. In our calculations,

the loss (3) was included in the threshold condition. As a result, the electron concentration in the active QW, N_2, is unclamped and changes with the injection current, so that the loss (3) is compensated by a corresponding increase of the optical gain in the main lasing transition.

Further enhancement of the modal index control is possible by increasing the confinement factor of the accumulation region, Γ, for instance, by using the injectorless QCL design [8, 9]. In regular QCL design, the modal index response to the carrier redistribution in the injector can be further increased by incorporating an additional intersubband polarization transition into the doped region of the injector. The frequency of this complementary transition and the frequency of the main polarization transition in the accumulation region should be located on the opposite sides from the frequency of the lasing transition *i.e.* they should be detuned in opposite directions. In this case, according to equation (2), the change of the refractive index due to depletion of the doped part of the injector will have the same sign as the refractive index change due to the carrier accumulation in the accumulation region, so that the total index change can be actually doubled. Note, that our tuning scheme with intersubband polarization transition can also accommodate the situation when the doped part of the injector is characterized by the residual quasi-3D dielectric response (free-carrier type absorption). In this case, the polarization transition in the accumulation region should be blue-shifted from the lasing transition so that the carrier redistribution between the doped and accumulation regions of the injector would lead to the refractive index change of the same sign. These more elaborate designs will be subject of a forthcoming publication.

In conclusion, we propose a new concept of cascade laser tuning based on electric charge accumulation outside the optically active layers. The outside charge accumulation allows above-threshold control over both the gain peak position and modal refractive index. This scheme provides a mechanism for ultra-wide quasicontinuous wavelength tuning in both intersubband (QCL) and interband (ICL) cascade lasers. In ICLs, the in-plane *intrasubband* carrier polarization in the accumulation region provides the necessary change of the TE modal refractive index. In QCLs, where the optical mode is TM-polarized with the electric field transverse to the QCL layers, the *intersubband* polarization transition is specially designed and incorporated in the accumulation region to achieve modal refractive index control.

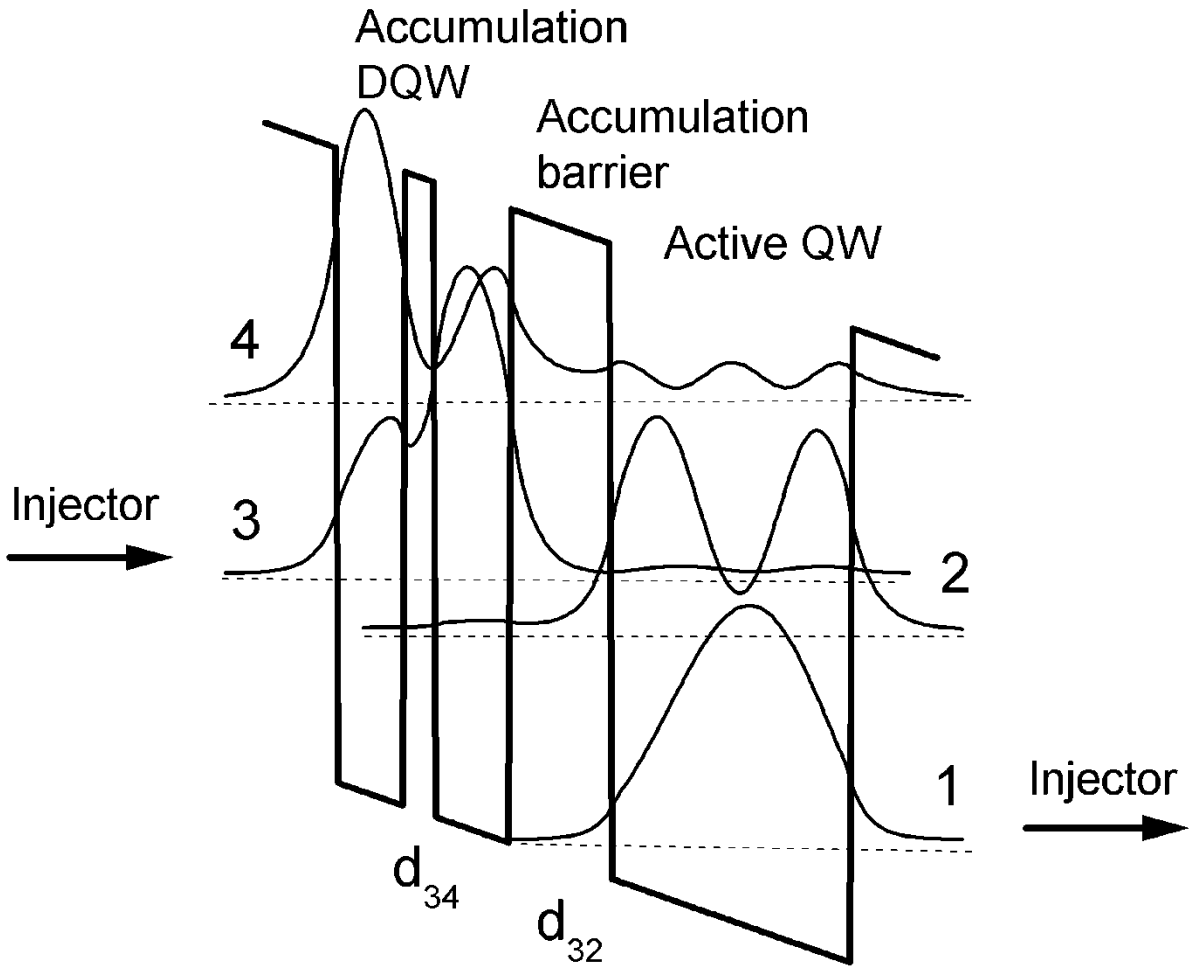

Figure 1.

Active region of a tunable QCL structure: optically active QW with intrawell lasing transition **2**–**1** and DQW accumulation region with polarization transition **3**–**4**. Accumulation barrier d_{32} controls the LO-phonon assisted injection transition **3**–**2**. Structure layout starting from the left accumulation QW to the optically active QW (DQW barrier and accumulation barrier show in bold): 2.3/**1.2**/2.7/**3.6**/8.5 nm. In an external field of 70 kV/cm the eigenstate energy separations $E_{32}/E_{34}/E_{21}$ are 40/127/150 meV with transition matrix elements for emission (z_{21}) and polarization (z_{34}) transitions 2.05 nm and 2.08 nm correspondingly. The sum of the 8-band envelope modulus squared for each eigenstate wave function is shown in the plot shifted to the eigenstate energy.

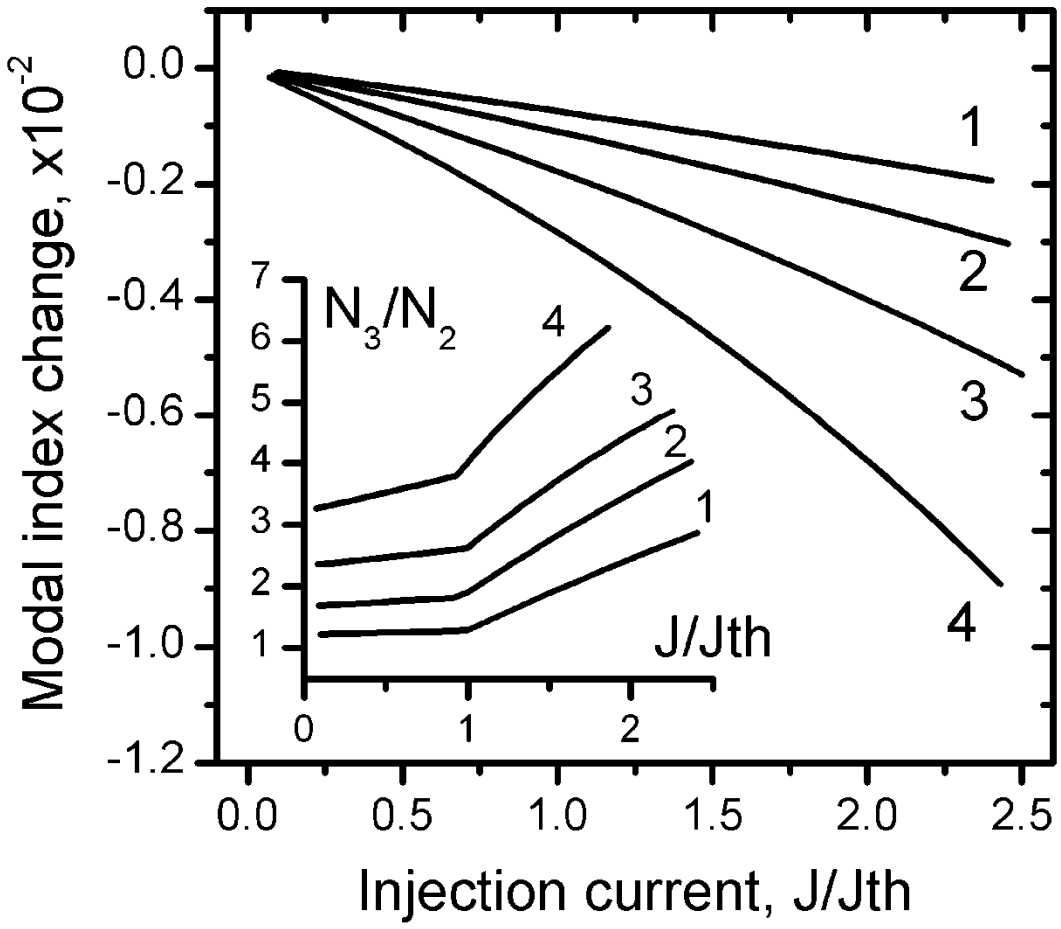

Figure 2

Modal index change due to intersubband polarization in DQW accumulation region of QCL structure presented in Figure 1. The curves are numbered with respect to increased tunneling barrier width d_{32} from 3.4 nm (curve 1) to 4.0 nm (curve 4). The injection current is normalized to the threshold value. The inset illustrates the charge build-up in the accumulation region showing the ratio of electron concentrations in the accumulation region (N_3) and in the upper lasing state (N_2). For structure 4 with d_{32} =4.0 nm these concentrations at threshold (J_{th}=1.4 kA/cm^2) were 4.4×10^{10} cm^{-2} and 1.1×10^{10} cm^{-2} respectively.

We demonstrated experimentally the effect of charge accumulation in a cascade laser structure using type II interband cascade laser. The *tunable interband c*ascade (IC) laser structure was grown by MBE on *p*-doped GaSb substrates. The active region of the laser is a cascade of 14 periods. Each period includes a digitally graded InAs/AlSb injector and InAs/$Ga_{0.8}In_{0.2}Sb$/GaSb type II heterostrucure, separated by a 4nm AlSb barrier. The widths

of the InAs and $Ga_{0.8}In_{0.2}Sb$ layers are 2.1nm and 3.1nm, respectively. The active area is sandwiched between InAs/AlSb superlattice claddings.

The $Ga_{0.8}In_{0.2}Sb$ layer is followed by a *p*-doped 5.8-nm GaSb QW which serves as a hole reservoir. The devices are fabricated as deep-etched mesas and soldered, epi-layer side up, to Au-coated copper mounts. The mesas 35 μm wide with 0.5-mm-long cavity lengths with both facets left uncoated. The mounts were attached to the cold finger of a liquid N_2 or He train cryostat. The emission was collected with the reflection optics and analyzed with an FTIR spectrometer. We compared the tuning characteristics of this structure with those of a regular 18-cascade IC laser **[10]**. The latter had an active region with type II W-like quantum wells and contained no special tunnel barriers for charge accumulation.

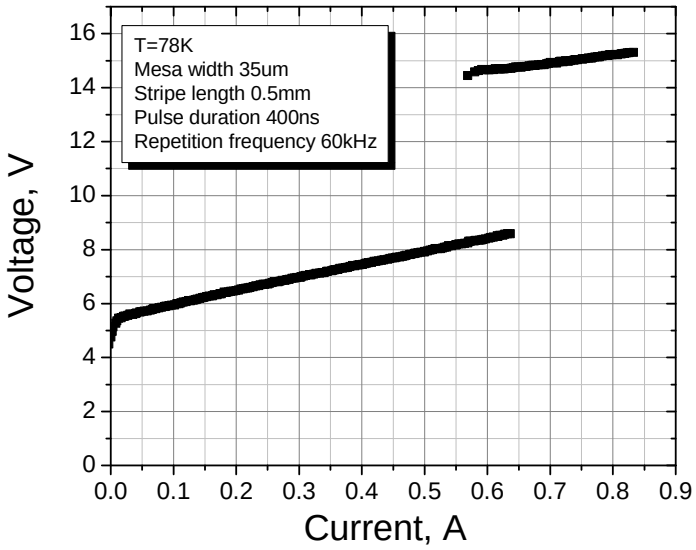

Figure 3
Current-voltage dependence of the tunable cascade laser

The current –voltage dependence of the structure is shown in the Fig.3. The experimental turn-on voltage is ~5.2 V and agrees well with the theoretical prediction (4.9V) for an ideal 14-period cascade structure. Calculation shows that 0,35 V voltage drop per each injector region provides for injector level alignment. For 56 nm injectors this corresponds to the turn-on internal electric field of ~ 65 kV/cm. As the bias current reaches ~ 650mA, the voltage jumps from ~8.5V to ~14.5V. There is no such a jump in the regular IC laser. This effect indicates to switching into another conducting state and may be a consequence of the charge build up in the accumulation quantum well. The switching is reversible and the bias current can be increased further after the voltage jump until the electrical breakdown of the dielectric separating the upper metal contact from the substrate occurs. A possible explanation of this behavior is that at higher bias current the charge accumulation and subsequent voltage drop leads to the energy alignment of the accumulation level and the second subband of the InAs/GaInSb laser quantum well. According to calculations, this subband is ~0.5eV higher than the upper lasing level. The width of the tunnel barrier 4 in our design was chosen 4 nm which ensures the alignment of the accumulation level 3 and upper lasing level 2 at turn-on

voltage (see Fig. 1). As the charge builds up in the accumulation well this alignment breaks due to voltage drop across the barrier. This does not necessarily mean immediate disruption of carrier injection into the upper laser level: the inelastic tunneling processes may be effective enough to keep proper injection rate [4]. However, as the energy misbalance between accumulation and upper lasing levels increases, the inelastic tunneling processes may become less effective and the net tunnel rate may decrease in spite of progressing carrier density buildup in the accumulation well. Enforcing the bias current at these conditions may provide a positive feedback for carrier accumulation and, as a result, uncontrollable increase of the voltage drop until a higher energy state in the type II quantum well will be aligned with the accumulation level. Assuming that this is the second subband in the InAs/GaInSb well, we can estimate the total voltage jump as ~7V for a 14 cascade structure. This agrees well with the observed jump of ~6V.

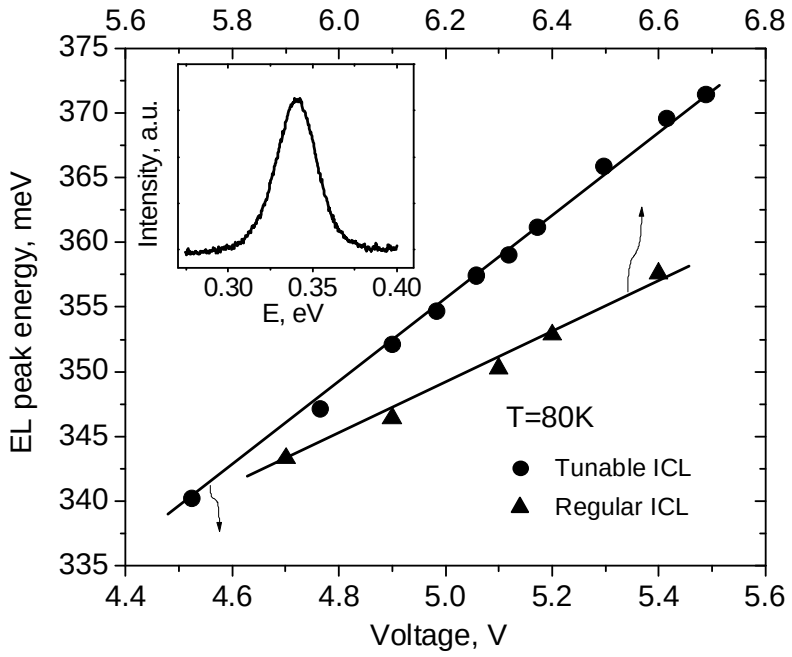

Figure 4
The dependence of the electroluminescence (EL) quantum energy on the bias voltage for a regular IC laser (triangles) and tunable IC laser (circles). The inset shows the EL spectrum at low bias current.

The electroluminescence (EL) spectrum at low current is shown in the inset of Figure 4. The emission quantum energy is 0.34 eV agrees with the theoretical prediction (0.32eV). The EL spectral maximum energy increases linearly with the bias voltage. Since the dependence is measured in the sub-threshold pumping region, the linear shift can be attributed to the Stark effect that results from charge accumulation in the type II quantum wells of the laser active area. A similar effect has been observed in a regular interband cascade laser (see Fig. 4). The effect is weaker in a regular IC laser due to the lower sensitivity of subband energies in a W-like quantum well with respect to charge accumulation.

The optical gain spectra measured with Hakki-Paoli technique are presented in Fig. 5

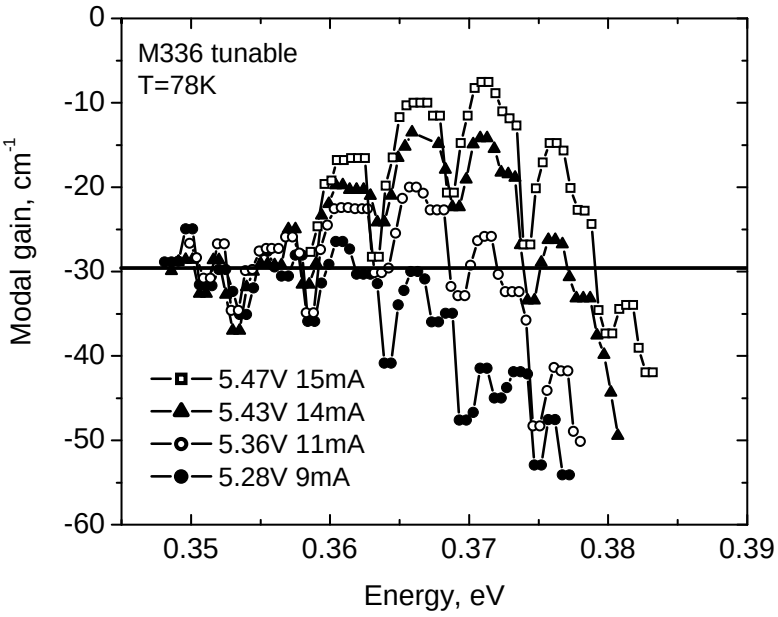

Figure 5
Modal gain spectra of the tunable laser at different bias currents

The modulation of the gain spectra indicates the presence of the substrate or "leaky" modes [11]. The effect also reveals as modulation of the amplified spontaneous emission (ASE) spectra and mode grouping in the lasing spectra. The observed threshold current density is 91 A/cm^2 at 80 K. The lasers demonstrates cw operation up to 120 K and pulsed operation up to 200 K (pulse duration = 400 ns, duty cycle = 2.4%). The external quantum efficiency is ~250% (80K). The internal loss is ~ 10cm^{-1} (Fig. 5).

Amplified spontaneous emission and lasing spectra of both the tunable and the regular IC lasers are shown in Figure 6. In the regular laser, in spite of the ASE blue shift, the laser line spectral position is stable up to high bias currents (~ 220 x threshold values). This is as expected from the pinning of concentration and, hence, of electric field in the active area quantum wells.

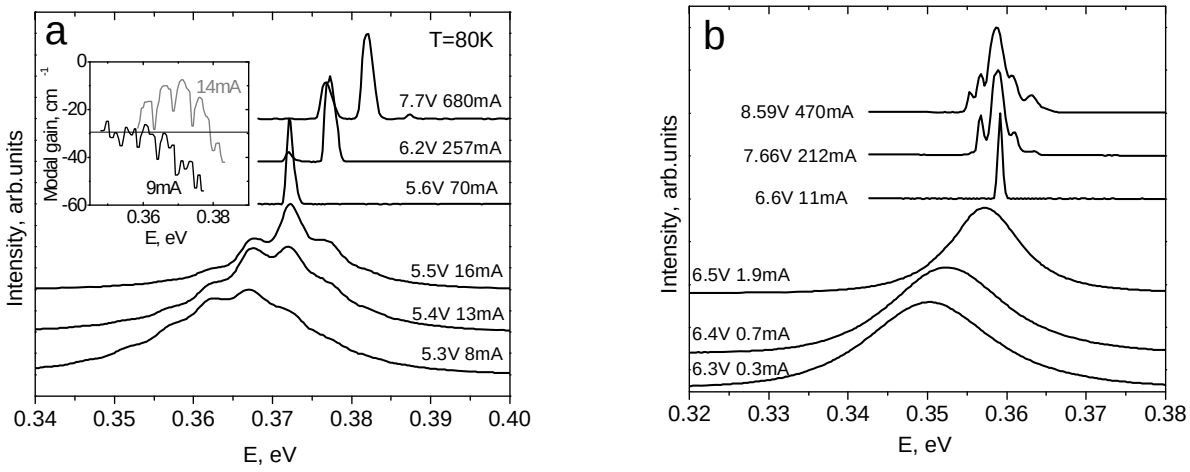

Figure 6
ASE and laser spectra of the tunable IC laser (a) and regular IC laser (b) at different bias currents. The inset in the panel (a) shows the modal gain spectrum of the tunable IC laser

The lasing spectrum of the tunable laser (see Fig. 6a, three upper curves) demonstrates a clear blue shift. The periodic modulation of the ASE spectrum in the tunable laser is consistent with the observed strong modulation of the modal gain spectrum with the same period (see Fig. 5 and Fig. 6a, inset). The spectral positions of the gain maxima and minima are determined by the substrate thickness as well as the effective refraction indices of the active area, claddings and substrate. The dependence of these positions on the bias current is weaker than the direct Stark shift of the gain spectrum. As the bias current increases, the material gain curve shifts with respect to the modulation extremes and consequently, the modal gain maximum shows a discrete blue shift with the increment equal to the leaky mode modulation period. This behavior takes place at the pumping level far higher than the laser threshold. The lasing spectrum of the tunable laser demonstrates a clear blue shift at increasing bias current. The rate of this shift with respect to the bias current (and voltage) is slower than the rate of ASE tuning in the subthreshold region (approximately 5 mEV/V vs. 30 meV/V). This indicates an abrupt change in the tuning mechanism as the bias current exceeds the laser threshold. In the subthreshold regime, the wavelength shift is determined primarily by the carrier accumulation in the optically active quantum wells and is related to the corresponding increase of the internal electric field in the type–II heterojunction. After the laser threshold has been reached, the wavelength tuning becomes determined by the charge buildup in accumulation quantum well 3, which, in turn, depends on the electron tunneling rate through barrier 4. The change in the tuning rate above the threshold indicates that, in the present design, the rate of charge accumulation in quantum well 3 is lower than that in the optically active quantum wells below the threshold. Figure 6 demonstrates the laser spectrum shift recorded throughout the whole range of the injection current (1-42 threshold values) without noticeable saturation. The maximum value of the laser emission tuning range is 15 meV or 120 nm (Figure 7).

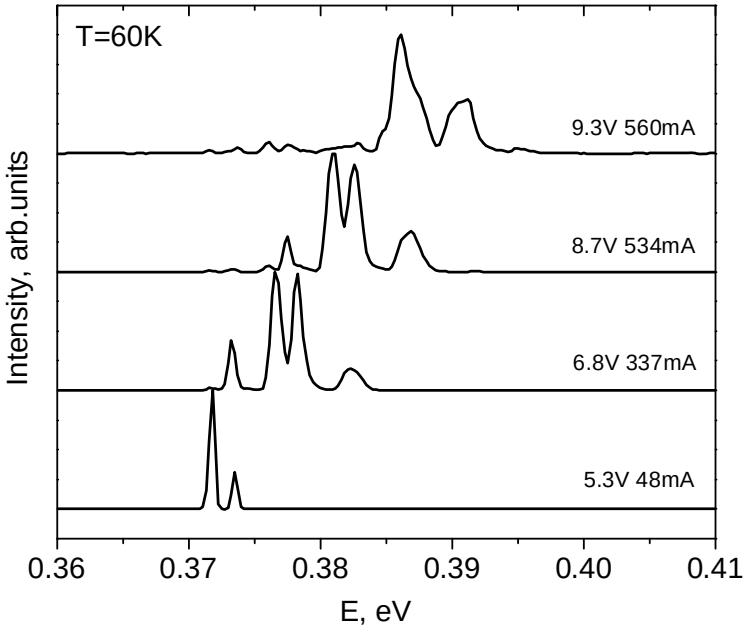

Figure 7
Lasing spectra of the tunable IC laser at different values of the injection current.

One of the principal advantages of the presented tuning scheme in comparison with temperature tuning is the possibility of fast wavelength modulation. To show the potential of the Stark tuning for high speed applications we measured the frequency response of the laser tuning. For this we combined the above-threshold dc bias component with ac bias component. The frequency of the ac component was varied in the range 0.01-2GHz. As soon as the bias modulation period is larger than the tuning response time of the laser, the laser spectrum shape will be changing in time with the bias. Since the spectrometer response time is larger than the bias modulation period in the whole modulation frequency range, the measured spectrum is the result of time averaging over all spectral shapes corresponding to the bias values within the modulation amplitude. As the bias modulation period becomes much smaller than the laser tuning response time, the laser wavelength is not affected by the bias modulation and the measured spectrum corresponds to dc component of the bias. Registering the change of the laser spectrum shape with the bias modulation frequency we can estimate the tuning modulation bandwidth.

For the measurements of the frequency dependence of the wavelength tuning we used the 0.5mm long laser with the mesa width of 8um and threshold current of 6mA at 80K. The differential resistance of the laser at the given dc bias is 6.9Ohm. A high frequency 47Ohm resistor was connected in series with the laser for the cable impedance matching. The dc bias current was 31mA, the ac modulation amplitude was 50mA. At 31 mA the threshold the laser spectrum consists of the single line (further referred as line 1). As the bias current increases to ~ 40mA, another line (line 2) corresponding to the next “leaky mode maximum” appears due to gain curve shift. The presence of the line 2 in the time –averaged spectrum means that the tuning response time is shorter that the laser modulation period. At higher frequencies line 2 disappears

and the laser spectrum shape returns to that without modulation (fig 8). The relative amplitude of the second line as a function of frequency (fig. 8) provides a rough estimation for the modulation bandwidth. The sharp decrease of the line 2 intensity takes place at ~ 1.6 GHz. The vanishing of the line 2 means that the peak bias current decreased from 56mA to ~ 40mA so the modulation amplitude decreased ~2.5 times. The 3dB (1.41times) decrease takes place at lower frequencies (~1GHz).

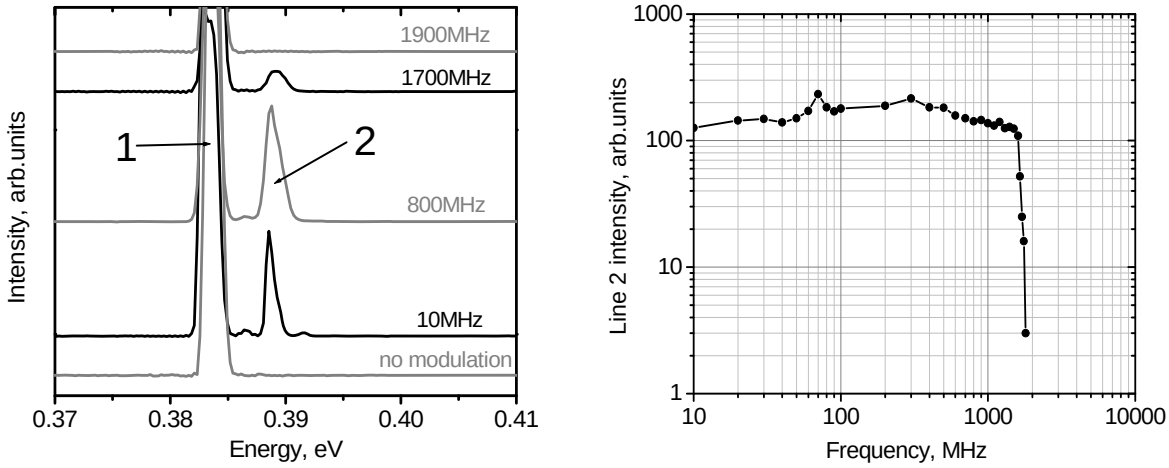

Figure 8
Lasing spectra at different modulation frequencies (right), frequency dependence of the intensity of line 2 (left)

The response time for the Stark wavelength modulation can be estimated as $\tau \sim RC$, where C is the capacitance of the device and R is the series resistance of the laser. The capacitance of the laser is the sum of the parasitic capacitance of the laser package C_P and internal capacitance of the laser structure C_L. To estimate C_L we consider each active area in each period as a plane capacitors connected in series by the conducting injectors. The electron and hole accumulation quantum wells represent the capacitor plates. The 8x500μm plates are separated by ~80A distance. Taking the dielectric constant ε ~12, we obtain ~ 4pF for the 14 cascade laser. At the series resistance of ~ 6.9Ohm the theoretical tuning bandwidth can be estimated as 36GHz. In our case the cutoff is most probably determined by C_P, which is estimated as ~ 20pF. With the total load resistance of 54Ohm it gives the cutoff frequency ~ 1GHz which is in good agreement with the experimental results [12].

We demonstrated high wavelength modulation rate of Stark tunable laser. This rate is not possible to reach using conventional thermal tuning.

A high power CW room temperature operated laser is a necessary technical platform to develop a single mode tunable device. Tunable Mid-IR semiconductor lasers emitting beyond 3μm are of special interest for chemical sensing, infrared countermeasures and pollution monitoring.

We report development of high power GaSb based quantum well (QW) laser operated in continuous wave (CW) mode above 3 μm at room temperature [13]. A major problem for this type of devices is lack of hole confinement in the active region QWs. This problem was successfully overcome by introduction of heavy compressive strain above 1% into InGaAsSb quantum well and utilization of the quinternary AlInGaAsSb barrier material. Introduction of the fifth component into the barrier alloy gives additional degree of freedom which allows control over the band offsets between barrier and quantum well material. The effect is illustrated in Fig. 9.

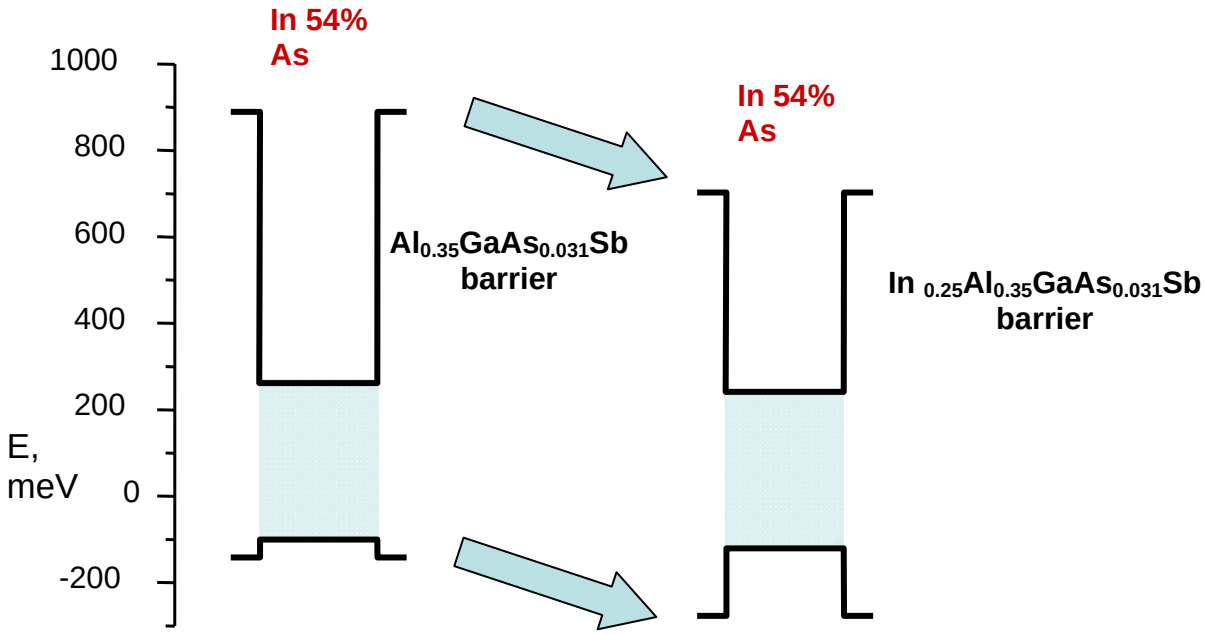

Figure 9

Effect of quinternary barrier on band offsets of the laser QW

The most important effect of the quinternary barrier is considerably improved hole confinement (to ~ 150meV). As a result CW operation of 3.36μm laser at room temperature was demonstrated [14]. Another important component of the QW laser design is strain of the quantum well material. We studied in detail the effect of QW strain on the laser performance. It was demonstrated experimentally that threshold current density of the lasers with 1.5% strained QWs was lower than this of the 1% strained devices by nearly two times [15] (Figure 10). Experiment shows that the reduction in threshold current density with increasing QW strain is related to the increase in differential gain and decrease in the transparency current density. Calculation of the QW energy spectra, density of states and optical gain were done in the frame of 8 band ***kp*** method. It was shown than improvement in the hole confined and reduction of the valence band effective mass in the devices with strained QWs reduces the threshold current density.

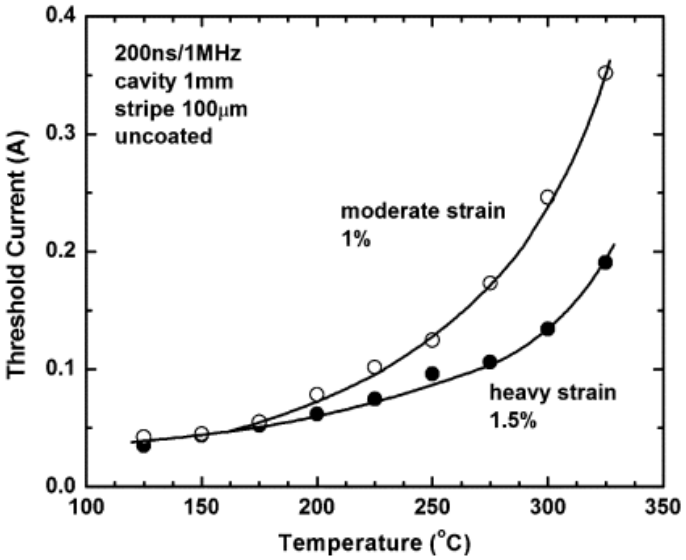

Figure 10

The effect of laser QW strain on the threshold current density.

Combination of quinternary barrier and laser QW strain being applied to 2.7 μm laser design lead to record performance characteristics of these devices. The lasers with 600mW CW output power at room temperature and peak power conversion efficiency of 10% were demonstrated [16] (Figure 11).

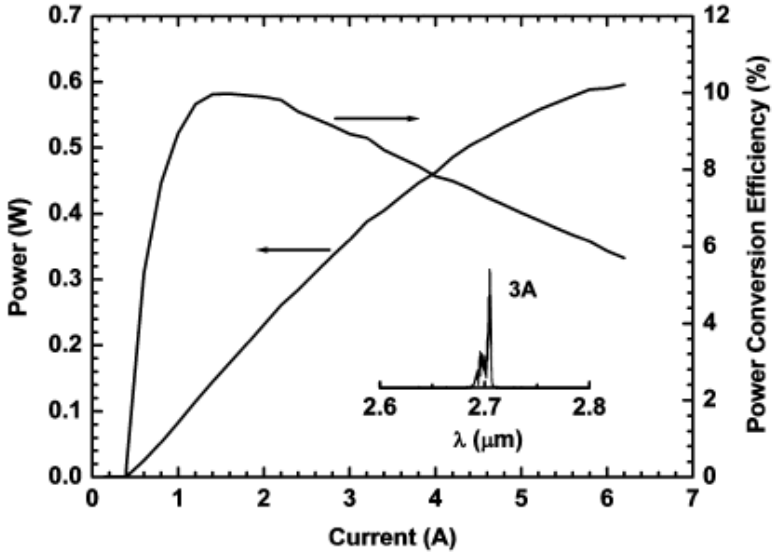

Figure 11

CW light –current and power conversion efficiency of 2.7μm laser. Room temperature.

Further improvement of the laser design was done by optimization of the waveguide width. The concept traditional “broadened waveguide“ design is based on the tradeoff between decreased

optical mode confinement factor and decreased optical loss due to lower overlap between optical mode and doped claddings. Our studies demonstrate that as the waveguide width was reduced from 1470 to 470 nm, the device performance considerably improved [17] (Figure 12).

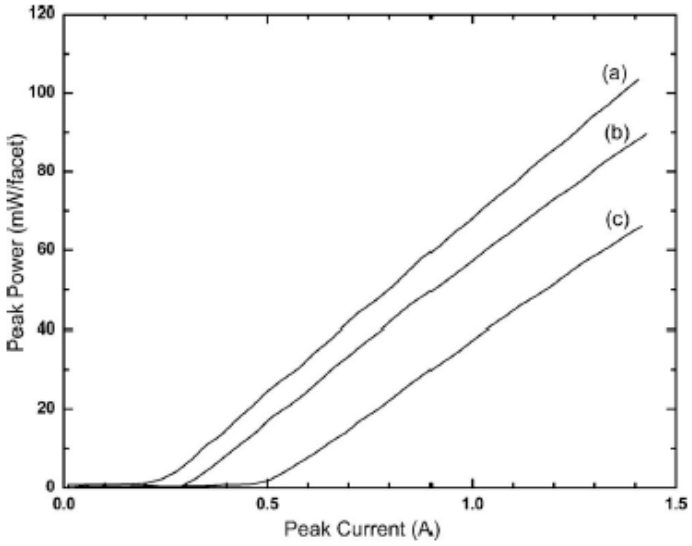

Figure 12

Light-current dependences for devices with different waveguide widths: (a) 470nm, (b) 1070nm, (c) 1470nm.

Again, the reduction of the threshold current density in the device with the shortest waveguide was due to increase of the differential gain. This may indicate to the importance of the carrier transport through the waveguide layer as another factor which determines laser waveguide width. Application of the optimized design allowed us to demonstrate 200mW of CW room temperature power at the wavelength of 3μm [17].

Fabrication of a single lateral mode laser is a necessary step in development of a tunable single mode semiconductor laser. We developed single lateral mode laser emitting at 3.15um at room temperature [18]. The mid-infrared laser heterostructures were grown by solid-source molecular beam epitaxy. In the laser active region there were three 1.65% compressively strained, 14-nm-wide, 40-nm-spaced InGaAsSb QW with nominal indium composition of 52%. Quinary $Al_{0.20}Ga_{0.55}In_{0.25}As_{0.24}Sb_{0.76}$ random alloy was utilized for barrier and waveguide. The width of the waveguide core from n-cladding to p-cladding was about 1120nm. The n- and p-claddings were $Al_{0.85}Ga_{0.15}As_{0.07}Sb_{0.93}$ doped with tellurium and beryllium, respectively. Doping level of the part of the p-cladding layer adjacent to waveguide was kept around $2x10^{17}$ cm^{-3} to reduce internal losses associated with free hole absorption.

Ridge waveguide lasers were fabricated using inductively coupled plasma (ICP) reactive ion etching technique at Jet Propulsion Laboratory. The etching was stopped at 350 - 400 μm before the end of the p-cladding to form shallow 12-μm-wide ridge lasers (Figure 13a). Estimated lateral effective index step was about 0.0013. For such a small refractive index step the 12-μm-wide ridge waveguide is expected to support only fundamental mode. The ridge lasers were cleaved to form 2-mm-long cavities and coated to reflect about 30% (neutral-reflection) and above 90%

(high-reflection), respectively. The devices were indium-soldered epi-side down on gold-coated polished copper blocks and characterized. Figure 13b shows the light-current-voltage characteristics and slow axis far field distribution measured at different temperatures.

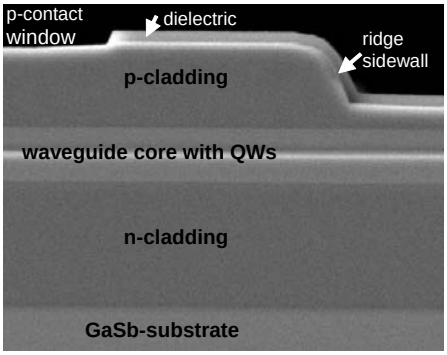

(a)

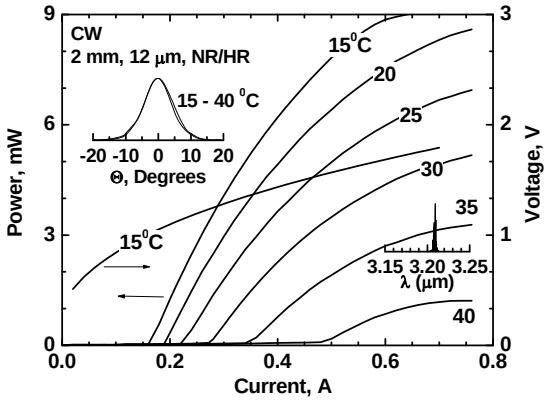

(b)

Figure 13

(a) SEM image of the front facet section the ridge waveguide laser; (b) CW light-current-voltage characteristics measured for 12-μm-wide 2-mm-long ridge waveguide lasers in temperature range from 15 to 40 ^{0}C. Inset shows the slow axis far field distributions measured at 15 and 40 ^{0}C. Laser spectrum at 0.4 A of CW current at 35 ^{0}C at heatsink is also shown.

Lasers operate in continuous wave regime up to 40 ^{0}C with diffraction limited output beam. The slow axis far field distribution remains nearly unchanged in temperature range from 15 to 40 ^{0}C. The measured FWHM is between 9 and 10 degrees. Model calculation predicted the FWHM about 9.4 degrees for a given ridge etch. The maximum power of 9 mW near 3.18 μm was achieved at the current of 0.65A at heatsink temperature of 15^{0}C. The devices generate above 1 mW of CW power at heatsink temperature of 40^{0}C (the operating wavelength is above 3.2 μm). The CW threshold current density was about 700 A/cm^2 at 15^{0}C and it rising up to 2 kA/cm^2. The voltage drop across laser heterostructure was below 2 V at the maximum output power level.

Summary of the most important results

- A novel scheme of rapid electrical tuning of the cascade lasers was proposed.
- The feasibility of the proposed scheme was justified experimentally. A tunable ICL laser with a record tuning range was demonstrated.
- The wavelength modulation bandwidth of the tunable ICL exceeding 1Ghz was demonstrated.
- Type I quantum well lasers with quinternary AlGaInAsSb waveguide were developed and fabricated. The devices operate CW at room temperature operation at the wavelength up to 3.4um.
- The patent on semiconductor light source with electrically tunable wavelength was awarded (app. # 20060056466).
- Single lateral mode laser operating CW at room temperature at the wavelength of 3.15um was demonstrated.
- The results are published in 9 papers and presented at international scientific conferences.

1. M. V. Kisin, M. Dutta, and M. A. Stroscio, "Eectron-phonon interactions in intersubband laser heterostructures," in *Advanced Semiconductor Heterostructures: Novel Devices, Potential Device Applications and Basic Properties*. vol. 28 Singapore: World Scientific, 2003, pp. 1-30.
2. M. V. Kisin, B. L. Gelmont, and S. Luryi, "Boundary-condition problem in the Kane model," *Physical Review B,* vol. 58, pp. 4605-4616, Aug 15 1998.
3. D .Westerfeld, S.Suchalkin, M.Kisin, G.Belenky, J.Bruno, R.Tober, “Experimental study of optical gain and loss in 3.4-3.6 mu m interband cascade lasers”, *IEE Proc.-Optoelectron.*, 150, 293 (2003).
4. M. V. Kisin, S. D. Suchalkin, and G. Belenky, "Stark effect tunable QCL," in *International Conference on Intersubband Transitions in Quantum Wells ITQW’2005*, North Falmouth, MA, USA, 2005.
5. S. Suchalkin, M. V. Kisin, S. Luryi, G. Belenky, F. J. Towner, J. D. Bruno, C. Monroy, and R. L. Tober, "Widely tunable type-II interband cascade laser," *Applied Physics Letters,* vol. 88, pp. 031103-3 (2006).
6. S.Suchalkin, M.V.Kisin, S.Luryi, G.Belenky, J.Bruno, F.J.Towner, R.Tober, "High-speed Stark wavelength tuning of mid-IR interband cascade lasers", *IEEE Photonic Technol. Lett.*, v.19, No5-8, 360 (2007)
7. L.Shterengas, G.Belenky, G.Kipshidze, and T.Hosoda, "Room temperature operated 3.1mm type I GaSb-based diode lasers with 80mW continuous-wave output power," *Appl. Phys. Lett.*, **92**, 171111 (2008).
8. L.Shterengas, G.Belenky, T.Hosoda, G.Kipshidze, and, S.Suchalkin "Continuous wave operation of diode lasers at 3.36μm at 12^{o}C," *Appl. Phys. Lett.*, **93**, 011103(2008).
9. J.Chen, D.Donetsky, L.Shterengas, M.Kisin, G.Kipshidze, and G.Belenky, "Effect of quantum well compressive strain above 1% on differential gain and threshold current

density in type-I GaSb-based diode lasers," *IEEE Journ. of Quant. Electron.*, 44, pp.1204-1210(2008).

Bibliography

[1] C. Gmachl, A. Straub, R. Colombelli, F. Capasso, D. L. Sivco, A. M. Sergent, and A. Y. Cho, "Single-mode, tunable distributed-feedback and multiple-wavelength quantum cascade lasers," *IEEE Journal of Quantum Electronics*, vol. 38, pp. 569-581, Jun 2002.

[2] J. Faist, F. Capasso, C. Sirtori, D. L. Sivco, A. L. Hutchinson, and A. Y. Cho, "Laser action by tuning the oscillator strength," *Nature*, vol. 387, pp. 777-782, Jun 1997.

[3] S. Suchalkin, M. V. Kisin, S. Luryi, G. Belenky, F. J. Towner, J. D. Bruno, C. Monroy, and R. L. Tober, "Widely tunable type-II interband cascade laser," *Applied Physics Letters*, vol. 88, pp. 031103-3, 2006.

[4] M. V. Kisin, S. D. Suchalkin, and G. Belenky, "Stark effect tunable QCL," in *International Conference on Intersubband Transitions in Quantum Wells ITQW'2005*, North Falmouth, MA, USA, 2005.

[5] M. V. Kisin, M. Dutta, and M. A. Stroscio, "Eectron-phonon interactions in intersubband laser heterostructures," in *Advanced Semiconductor Heterostructures: Novel Devices, Potential Device Applications and Basic Properties*. vol. 28 Singapore: World Scientific, 2003, pp. 1-30.

[6] M. V. Kisin, B. L. Gelmont, and S. Luryi, "Boundary-condition problem in the Kane model," *Physical Review B*, vol. 58, pp. 4605-4616, Aug 15 1998.

[7] I. Vurgaftman and J. R. Meyer, "Band parameters for III-V compound semiconductors and their alloys," *Journal of Applied Physics*, vol. 89, pp. 5815-5875, Jun 1 2001.

[8] M. C. Wanke, F. Capasso, C. Gmachl, A. Tredicucci, D. L. Sivco, A. L. Hutchinson, S. N. G. Chu, and A. Y. Cho, "Injectorless quantum-cascade lasers," *Applied Physics Letters*, vol. 78, pp. 3950-3952, 2001.

[9] N. Ulbrich, G. Scarpa, G. Bohm, G. Abstreiter, and M.-C. Amann, "Intersubband staircase laser," *Applied Physics Letters*, vol. 80, pp. 4312-4314, 2002.

[10] J.L.Bradshaw, N.P.Breznay, J.D.Bruno, J.M.Gomes, J.T.Pham, F.J.Towner, D.E.Wortman, R.L.Tober, C.J.Monroy, K.A.Olver, "Recent progress in the development of type II interband cascade lasers", *Physica E* 20, 479 (2004).

[11] D.Westerfeld, S.Suchalkin, M.Kisin, G.Belenky, J.Bruno, R.Tober, "Experimental study of optical gain and loss in 3.4-3.6 mu m interband cascade lasers", *IEE Proc.-Optoelectron.*, 150, 293 (2003).

[12] S.Suchalkin, M.V.Kisin, S.Luryi, G.Belenky, J.Bruno, F.J.Towner, R.Tober, "High-speed Stark wavelength tuning of mid-IR interband cascade lasers", *IEEE Photonic Technol. Lett.*, v.19, No5-8, 360 (2007)

[13] L.Shterengas, G.Belenky, G.Kipshidze, and T.Hosoda, "Room temperature operated 3.1mm type I GaSb-based diode lasers with 80mW continuous-wave output power," *Appl. Phys. Lett.*, **92**, 171111 (2008).

[14] L.Shterengas, G.Belenky, T.Hosoda, G.Kipshidze, and, S.Suchalkin "Continuous wave operation of diode lasers at 3.36μm at 12^{o}C," *Appl. Phys. Lett.*, **93**, 011103(2008).

[15] J.Chen, D.Donetsky, L.Shterengas, M.Kisin, G.Kipshidze, and G.Belenky, "Effect of quantum well compressive strain above 1% on differential gain and threshold current

density in type-I GaSb-based diode lasers," *IEEE Journ. of Quant. Electron*., 44, pp.1204-1210(2008).

[16] J.Chen, G.Kipshidze, L.Shterengas, T.Hosoda, Y.Wang, D.Donetsky, and G.Belenky, "2.7-μm GaSb-based diode lasers with quinary waveguide," *IEEE Journ. of Quant. Electron*., 44, pp.1204-1210(2009).

[17] T.Hosoda, G.Kipshidze, L.Shterengas, S.Suchalkin and, G.Belenky, "200mW type I GaSb based laser diodes operating at 3μm: Role of the waveguide width," *Appl. Phys. Lett.*, **94**, 261104(2009).

[18] J. Chen, T. Hosoda, G. Kipshidze, L. Shterengas, G. Belenky, “Single Spatial Mode Room Temperature Operated 3.15 μm Diode Lasers”, Electron. Lett. 46, v.5 (2010)